

SiC Micromachined Mach-Zehnder interferometer on Silicon for pressure sensor

G. Pandraud, L.S. Pakula, H.T.M. Pham*, P.J. French and P.M. Sarro*
Delft University of Technology, DIMES-EI, *DIMES-ECTM
P.O. box 5031, 2600 GA Delft, The Netherlands
E-mail: g.pandraud@ewi.tudelft.nl

Abstract— This paper describes an interferometric pressure sensor. The sensor is fabricated from a silicon carbide waveguide Mach-Zehnder integrated on a silicon substrate, and includes a micromachined membrane below a branch of the Mach-Zehnder. The analytical description takes into account the induced deflection of the membrane and the resulting mechanical elongation of the waveguide.

Keywords— photonics, silicon carbide waveguides, pressure sensor, silicon micromachining.

I. INTRODUCTION

Sensors based on optics and integrated optics feature a configuration without electrical wires, since no electrical supply is required on the location of measurements. This is particularly interesting in explosive atmosphere, or in an electromagnetic sensitive environment. We will present the fabrication process and preliminary results of an interferometric pressure sensor based on a Mach-Zehnder Interferometer (MZI) with a free standing micro-machined arm. An integrated pressure waveguide sensor on silicon is described, for instance, in [1]. The deformation of the membrane under pressure variation induces phase variation through elastooptic effects since the center of the waveguide is close to the edge of the membrane. The output intensity of the interferometer is a cosine function of the phase. Most of the interferometric sensors are built using Si_3N_4 or doped SiO_2 known for their excellent waveguiding properties and established fabrication process of the guided-wave devices.

SiC has recently attracted interests because of its good mechanical properties but moreover because of its resistance to harsh environment. We have demonstrated recently that it can also be a good candidate to guide light in the visible allowing then the design of attenuators [2] and the fabrication of vibration sensors [3]. This paper proposes an integrated optic pressure sensor using PECVD SiC waveguides. The sensor structure and the operating principal are described. The

sensor operation is analyzed to obtain its design concept. The fabrication process is described and preliminary results presented.

II. OPTICAL DESIGN OF INTERFEROMETER

Fig. 1 shows the basic device that consists of a guided-wave MZI on a $\langle 100 \rangle$ silicon substrate. Optical investigations on propagation losses of SiC waveguides have been reported in [3] and shown to be lower than 4 dB/cm. The rib waveguide considered in the optical investigation is shown in Fig.2. In order to design small devices, we performed measurement loss on bent waveguides with different radius. Fig. 3 presents the results obtained. As the losses measured for straight waveguides placed on the same chips are 3.5 dB/cm on average, we subtracted those losses and deducted the excess loss given by the curvature only. Losses can be low if the radius of curvature is kept equal or higher than 6 mm. For that radius the excess loss is found to be 0.5 dB/rad. By comparison previous pressure sensors designed using SiN are using 4 cm bend radius. The use of small radius is made possible thanks to the high confinement of the light in the waveguides. The refractive index of PECVD SiC is found to be 2.5589 at 0.633 μm .

MultiMode Interference (MMI) devices are used as 50% power splitter at the input and the output of the device. They are 12 μm wide, 425 μm long and are shown in Fig. 4. They are independent in polarization.

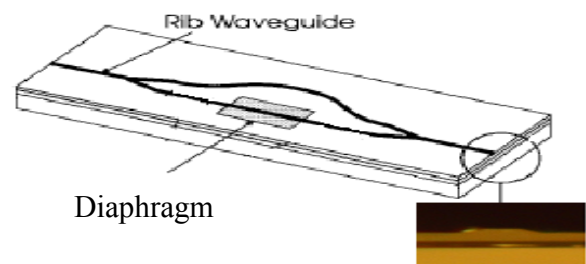


Figure 1. Scheme of the Mach-Zehnder pressure sensor integrated on silicon.

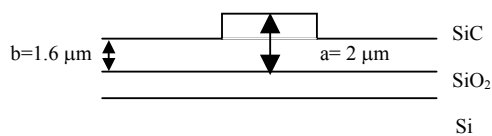


Figure 2. Description of the rib waveguide. The guiding layer is a 2 μm thick silicon carbide layer deposited by PECVD. The waveguide is 4 μm wide.

In that case the refractive index method gives a slab (region of thickness b) effective index of 2.5521291 and a rib effective index of 2.554468 (region of thickness a). The contrast of the waveguide (relative to the surrounding medium) is then $\Delta = 0.1\%$.

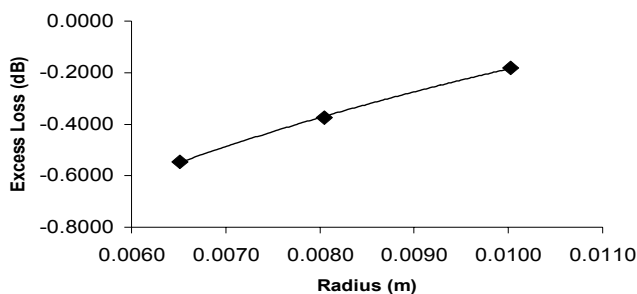


Figure 3. Measured bending loss in 4 μm wide SiC rib waveguides.

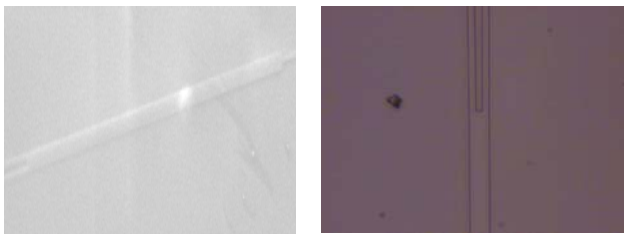


Figure 4. Top view of the MMI used as a power splitter and its branching region.

The transmission losses of the design interferometer, with bend radius of 6 mm, are 5 dB (the fresnel and coupling being found from the cut back measurements performed on straight waveguides and subtracted here). The total size of the device is 1 cm. Between the two 50% couplers a straight section of 0.18 cm is added. That's where the membrane will be realized on one arm.

III. FABRICATION

A SiO_2 layer is first formed by thermal oxidation on both sides of the wafer yielding a thickness of 1 μm. We have shown in [2] that such a thickness was required to

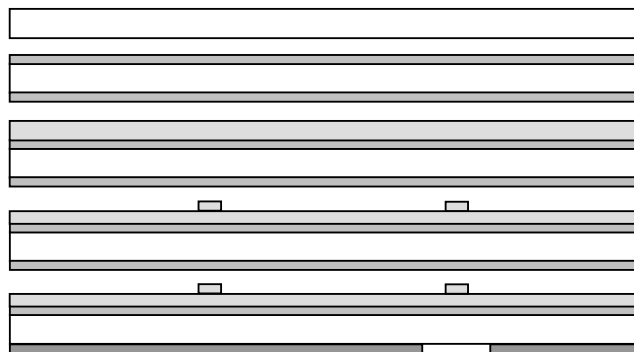
provide a good optical isolation. Then a 2 μm thick PECVD SiC layer is deposited. To ensure a stress free structure we anneal the samples at 500 °C. That allows also the waveguide to be Polarization Dependent Loss free [4]. The back side oxide is then removed and replaced by a 2 μm thick PECVD SiO_2 . This layer is then selectively etched and used as a mask for the following cryogenic process.

To make one arm of the interferometer free standing we back-side etched the silicon using Induce Coupled Plasma (ICP) etching process at cryogenic temperatures [5]. The experiments have been performed in a high density ICP reactor (Alcatel MET). It has independent control of radical and ion fluxes and substrate temperature. Etching is done with SF_6 as the reactive gas, because SF_6 gives the highest etch rates. Gas flows are in the range of 50-500 sccm, which leads to pressures of 0.5-5 Pa. In the cryogenic process O_2 is added as a sidewall passivating agent, typically about 10%. Quartz liners that protect the substrate against contamination from the reactor walls are slowly consumed by the plasma and form a source of oxygen.

Etching was performed using the following plasma parameters: 400 sccm SF_6 flow, 12 sccm O_2 flow, 2000W rf power and a substrate bias of -40V. The average etch rate was ~7 microns/min. These process settings proved to be adequate for etching holes and open structures.

The full process flow is shown in fig. 3. The devices have been made and are currently under investigation. In order to test them a cuvette will be glued on the back side of the interferometer. Once the cavity then formed is perfectly sealed we will change the pressure by creating slowly the vacuum.

Figure 4 shows a top view of the Mach-Zehnder when etched into the SiC layer. When we test this device in an optical bench use to characterize the optical losses of the SiC waveguides we find that the transmission before the membrane is etched is 3.5 dB. Figure 5 shows a side view of the through wafer etching process used here to produce the circular membranes in recess [6].



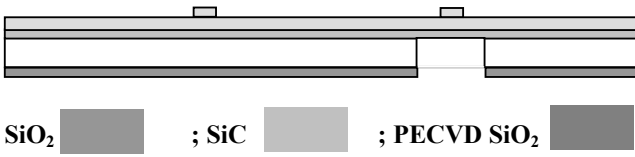


Figure 5. Main steps of the technological fabrication process of the device.

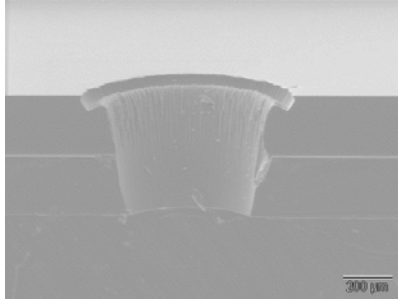


Figure 6. Through wafer etching test using an ICP etching process at cryogenic temperature.

IV. PRINCIPAL OF OPERATION

From mechanical considerations, we consider the optical path variation induced by the geometrical deformation of the membrane as a function of the pressure P . We use the analytical expressions given in [7] and [8]. We also use the hypothesis, which is verified when using ICP etching process that the membrane is rectangular, of length l and width w , and that the thickness e is weak compared with the length and the width. In the model, the thickness is assumed to be uniform. The four edges of the membrane are assumed to be clamped rigidly. We use the hypothesis of elastic deformations, which is usually met in SiC [8] membrane. We neglect the effect of remaining stress in the layer as low stress layer is used here. Then, we can easily express the pressure P as a nonlinear function of the deflection h_0 induced at the centre point of the membrane:

$$P = Ee^3 h_0 / a^4 (1 - \nu) [1/12 \alpha (1 + \nu) + C h_0 / e^2] \quad (1)$$

with E the young's modulus and ν the Poisson's ratio. α is a coefficient given by Timoshenko [9], depending on the ratio l/w . In our case we choose $l/w=2$ and $\alpha = 2.54 \times 10^{-3}$. In [6], Tabata gives an analytical expression of the coefficient C . in our case with $m=0.5$, $C=10.94$. We can now assess the phase shift produced by a pressure P . We consider only the expansion of the waveguide due to the membrane deformation. Experiments confirm in the following that the variations

of the path difference due to elasto-optic effects are negligibly small compared with the geometrical length variation of the waveguide. We first express the relation between the excess length and the deflection at the center of the membrane to the optical path variation. The shape of the deflection $h(x)$ of the membrane along the axis of propagation is expressed as :

$$h(x) = h_0 \cos^2(\pi x / l) \quad (2)$$

The excess total optical path difference produced by the membrane can be derived from (2), yielding for weak deformations:

$$\Delta P = (n_{\text{eff}} \pi^2 / 4) * (h_0^2 / l) \quad (3)$$

There is a tradeoff between the width w and the length of the membrane to insure a maximum deflection h , and hence a maximum phase variation. The deflection is shown to be optimal as $l/w=2$.

V. SIMULATION RESULTS

The output optical signal according to the pressure is given by

$$I(P) = I_0 / 2 [1 + 0.5 \cos(\Delta P)] \quad (4)$$

where I_0 is the optical power of the source.

a) Effect of the thickness layer:

In order to optimize or design we followed the effect of different parameters. For example if when the thickness of the SiC film decrease the sensitivity is drastically improved.

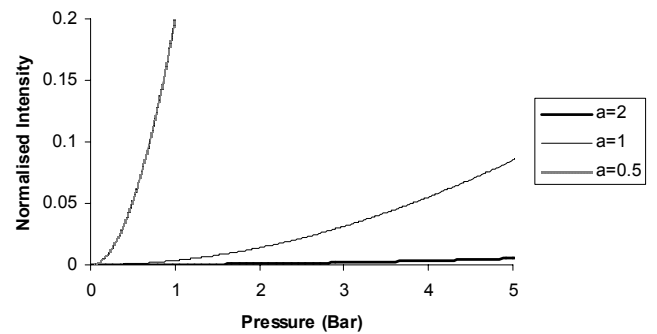


Figure 7. Simulated output intensity of the interferometer when a (thickness of the SiC film) varies.

For small thickness values the difference in effective index between the slab region (thickness b in fig. 3) and the rib region is bigger leading to a smaller ΔP .

It is interesting to notice here that a thin dielectric layer of high refractive index (i.e. SiC) offers a sensitivity while used in evanescent wave sensors [9]. The present interferometer will be then also tested as a biosensor (in that case it is not the change of the pressure which will generate the change of n_{eff} but the change of the index of the covering layer (water, air....)).

b) Effect of the waveguide shape:

The remark made in the previous section remains valid here. The higher the confinement (i.e. b/a small) the lower n_{eff} .

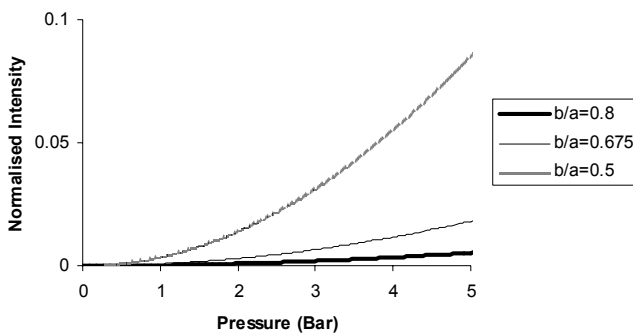


Figure 8. Simulated output intensity of the interferometer when the ratio b/a (etch depth) varies.

c) Effect of the membrane number:

In order to improve the sensitivity [10] proposed to use more than one membrane. In that case (3) becomes for two consecutive membranes:

$$\Delta P = (n_{\text{eff}} \pi^2 / 4) * (2h_{01}^2 / l_1) \quad (5)$$

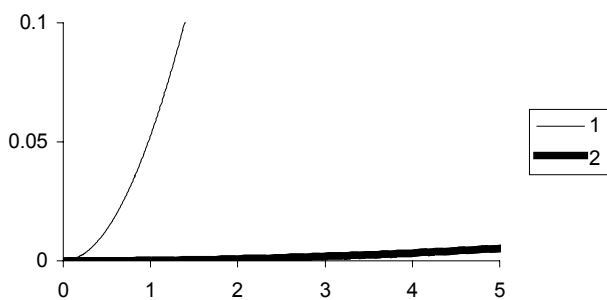


Figure 9. Simulated output intensity of the interferometer when one and two consecutive membranes are considered.

If a second membrane is added the device will then be longer.

VI. CONCLUSION

We presented the design and the fabrication process of a pressure sensor using SiC waveguides. The response of the sensor can be properly adjusted according to the desired specifications. In our case and based on prior loss results, we fabricated an interferometer with 2 μm thick SiC layer etched down to 1.6 μm . The expected sensitivity is 2.5%/bar.

VII. ACKNOWLEDGEMENT

The authors wish to thank G. Craciun and engineers from the Delft Institute of MicroElectronics and Submicrontechnology (DIMES) for technical assistance. This project is supported by the Dutch Technology Foundation, STW (project DMF. 5103).

REFERENCES

- [1] M. Ohkawa, M. Izutsu and T. Sueta, *Appl. Opt.*, vol. 28, no 23, pp. 5153-5157, 1989.
- [2] G. Pandraud, H. Yang, L.S. Pakula, H.T.M. Pham, P. J. French and P.M. Sarro, *Proceedings of SAFE 2003*, pages 613-634, Veldhoven, The Netherlands, 2003.
- [3] G. Pandraud, L.S. Pakula, H.T.M. Pham, P. J. French and P.M. Sarro, *Proceedings of Eurosensors 2004*, pages 24-25, Rome, Italy, 2004.
- [4] G. Pandraud, H.T.M. Pham, P. J. French and P.M. Sarro, *Optical Materials*, submitted.
- [5] G. Craciun, M. Blauw, E. van der Drift, P.M. Sarro and P. J. French, *J. of Micromechanics and Microengineering*, 12, pp. 390-394, 2002.
- [6] D.H.B. Wicaksono, G. Pandraud, G. Craciun, J.F.V. Vincent and P.J. French, *Proc. MME*, pp. 80-83, Leuven, Belgium, 2004.
- [7] O. Tabata, K. Kawabata, S. Sugiyama and I. Igarshi, "Mechanical property measurement of thin films using load-deflection of composite rectangular membranes", *Sensors and Actuators*, vol. 20, pp. 135-141.
- [8] E. Bonnotte, P. Delobelle, L. Bornier, B. Trolard and G. Tribillon, "Mise en oeuvre de deux methods interferometriques pour la caracterisation mecanique des fines minces par l'essai de gonflement. Applications au cas du silicium monocristallin", *J. de Physique III*, vol.5, pp. 953-983, 1995.
- [9] O. Parriaux, P.V. Lambeck, H.J.W.M. Hoekstra, G.J. Veldhuis and G. Pandraud, *Optical and Quantum Electronics*, vol. 32, pp. 909-921, 2000.
- [10] H. Porte, V. Gorel, S. Kiryenko, J.P. Goedgebuer, W. Daniau and P. Blind, *Journal of Lightwave Technology*, vol. 17, pp. 229-233, 1999.